ROYAL SOCIETY
OF CHEMISTRY

EDGE ARTICLE

Check for updates

All publication charges for this article
have been paid for by the Royal Society
of Chemistry

Direct hydrogen selenide (H₂Se) release from activatable selenocarbamates†

Turner D. Newton, ‡[a] Keyan Li, ‡[a] Jyoti Sharma, [b]
Pier Alexandre Champagne *[b] and Michael D. Pluth *[a]

Hydrogen selenide (H₂Se) is a possible bioregulator, potential gasotransmitter, and important precursor in biological organoselenium compound synthesis. Early tools for H₂Se research have benefitted from available mechanistic understanding of analogous small molecules developed for detecting or delivering H₂S. A now common approach for H₂S delivery is the use of small molecule thiocarbamates that can be engineered to release COS, which is quickly converted to H₂S by carbonic anhydrase. To expand our understanding of the chemical underpinnings that enable H₂Se delivery, we investigated whether selenocarbamates undergo similar chemistry to release carbonyl selenide (COSe). Using both light- and hydrolysis-activated systems, we demonstrate that unlike their lighter thiocarbamate congeners, selenocarbamates release H₂Se directly with concomitant isocyanate formation rather than by the intermediate release of COSe. This reaction mechanism for direct H₂Se release is further supported by computational investigations that identify a $\Delta\Delta G^{\ddagger} \sim 25$ kcal mol^{-1} between the H₂Se and COSe release pathways in the absence of protic solvent. This work highlights fundamentally new approaches for H₂Se release from small molecules and advances the understanding of reactivity differences between reactive sulfur and selenium species.

Introduction

Small molecule bioregulators play important roles in diverse biological processes. Of such molecules, small polyatomic examples, such as NO, H₂S, and CO have joined a class of compounds often referred to as 'gasotransmitters' that play key roles in physiological function, disease progression, and signaling pathways.[1–6] Each of these gasotransmitters has attracted significant work aimed at developing chemical tools for detection and delivery of these small molecules in complex biological environments.[7–14] More recently, hydrogen selenide (H₂Se) has attracted increased attention as a possible bioregulator, potential gasotransmitter, and important precursor in biological organoselenium compound synthesis.[15–18] Moreover, H₂Se is a likely reactive intermediate in initial reduction of dietary selenium sources to form selenophosphate, en route to downstream selenium-containing biomolecules including selenocysteinyl-tRNA$_{Sec}$, selenouridine, and selenosugars.[19,20]

aDepartment of Chemistry and Biochemistry, Materials Science Institute, Knight Campus for Accelerating Scientific Impact, Institute of Molecular Biology, University of Oregon, Eugene, Oregon, 97403-1253, USA. E-mail: pluth@uoregon.edu

bDepartment of Chemistry and Environmental Science, New Jersey Institute of Technology, Newark, New Jersey, 07103, USA. E-mail: pier.a.champagne@njit.edu

† Electronic supplementary information (ESI) available: NMR spectra and full computational details. See DOI: https://doi.org/10.1039/d3sc01936e

‡ These authors contributed equally to this work.

Initial tools for H₂Se delivery have benefited from earlier work on H₂S donor development that provided a strong mechanistic background for understanding how to engineer small molecules to release H₂Se in different environments (Fig. 1).[9,10,21] For example, building from the analogous GYY4137[22] and FW1256[23] platforms that rely on P=S hydrolysis for H₂S delivery, we developed the P=Se motifs TDN1042[24] and 2AP-PSe[25] that are hydrolyzed to release H₂Se. Similarly, Yi and co-workers adapted arylthioamides, which release H₂S upon reaction with cysteine, to develop arylselenoamides that release H₂Se upon activation by cysteine.[19] Recent examples of H₂Se donors have also developed new chemistry not based on prior H₂S donor platforms, including work by Yi and co-workers on cysteine-mediated H₂Se release from selenocyclopropenes[19] and by Lukesh and co-workers on the base-mediated H₂Se
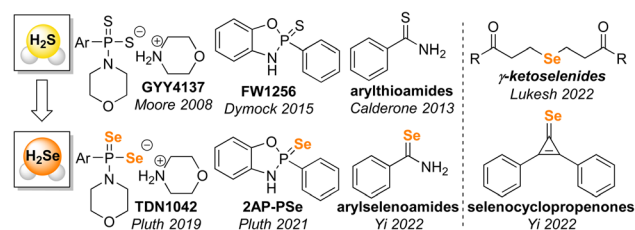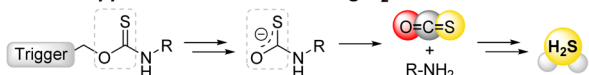

Fig. 1 Overview of selected H₂Se donors inspired by prior H₂S releasing motifs and associated H₂Se donors demonstrated to release H₂Se directly.

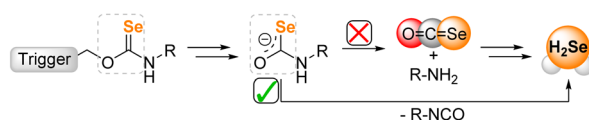**(a) General Approach for COS-Releasing H₂S donors**

(b) This work

Fig. 2   (a) General approach for COS release from thiocarbamates as precursor for H₂S delivery. (b) Summary of this work highlighting that selenocarbamates release H₂Se directly rather than requiring intermediate COSe formation.

release from γ-ketoselenides.[26] Taken together, these prior examples of H₂Se delivery highlight that H₂Se donor are poised to not only leverage previous sulfur-based chemistry but also identify new reactivity that differs from its lighter chalcogen congener.

A recent area of H₂S donor expansion has grown from the discovery that small molecules that release carbonyl sulfide (COS) can function as H₂S donors due to the rapid conversion of COS to H₂S by the ubiquitous enzyme carbonic anhydrase (CA).[27] One benefit of this class of COS-based H₂S donors is that many of the scaffolds can be engineered to only release COS/H₂S in response to a specific trigger. Selected examples of such prior triggering motifs include reactive oxygen species,[28–31] light,[32–34] changes in pH,[35,36] and enzymatic activation.[37–39] Building from the potential analogous reactivity between S- and Se-containing donor platforms, we wanted to determine whether common motifs used to release COS/H₂S could be repurposed to release COSe/H₂Se by substitution of S for Se atom. In addition to advancing the fundamental chemistry of reactive selenium species (RSeS), if such donors were to release COSe and/or H₂Se they would significantly expand the versatility of triggered RSeS release. Our work here, which is supported by both experimental and computational data, demonstrates that activatable selenocarbamates release H₂Se directly rather than through intermediate COSe generation, which not only highlights fundamental differences between S and Se chemistry, but also enables a direct and modifiable approach for H₂Se delivery (Fig. 2).

Results and discussion

Our first goal was to prepare a selenocarbamate (SeCM) that was stable until activated by a specific external stimulus. Based on our prior work with light-activated thiocarbamates containing the photocleavable o-nitrobenzyl group as COS/H₂S donors,[32] we focused on the analogous selenocarbamate motifs. Using a similar synthetic approach as for the thiocarbamates, we treated the p-fluorophenyl isoselenocyanate with 2-nitrobenzyl alcohol in THF at 0 °C in the presence of NaH to afford the desired selenocarbamate product (PhotoSeCM, Scheme 1). The ^{77}Se NMR spectrum of the product showed a major peak at 278 ppm, which is consistent with formation of the O-alkyl
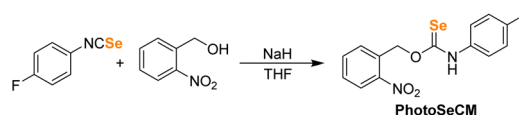
Scheme 1   Synthesis of o-nitrobenzyl selenocarbamates.

selenocarbamate. We note that earlier work with the parent PhNCSe starting material showed either partial or full isomerization of the selenocarbamate product to the Se-alkyl selenocarbamate upon purification by SiO₂ chromatography, which was supported by a shift in the ^{77}Se NMR spectrum from 281.2 ppm to 462.2 ppm. This downfield resonance is consistent with previously reported Se-alkyl selenocarbamate [77]Se shifts and suggests that these compounds may undergo a Newman–Kwart[40,41] rearrangement promoted by silica gel. To avoid using mixtures of the O- and Se-alkyl selenocarbamates, we optimized the purification and isolation procedure of PhotoSeCM to include recrystallization rather than chromatography and allow for isolation of a single isomer.

With PhotoSeCM in hand, we next investigated the product formation after photoactivation. To simplify the overall reaction conditions, we investigated the reaction in THF with the goal of limiting hydrolysis of potential reaction products. Moreover, monitoring the ^{19}F NMR spectrum of the reaction allows for identification of major p-fluoroaniline based reaction products. Upon irradiation at 365 nm, we expected that the primary products would be COSe, p-fluoroaniline, and 2-nitrosobenzaldehyde, however this was not the case. When monitoring the ^{19}F NMR spectrum of the reaction, we observed consumption of the PhotoSeCM signal at −117 ppm but failed to observe the expected p-fluoroaniline product at −130 ppm (Fig. 3). Rather, we observed a new product peak at −123 ppm corresponding to formation of p-fluoroisocyanate, which was confirmed by comparison to an authentic sample. Formation of the isocyanate product suggests that COSe release does not occur upon irradiation, but rather that H₂Se/HSe⁻ is released directly from the selenocarbamate through a pathway that is
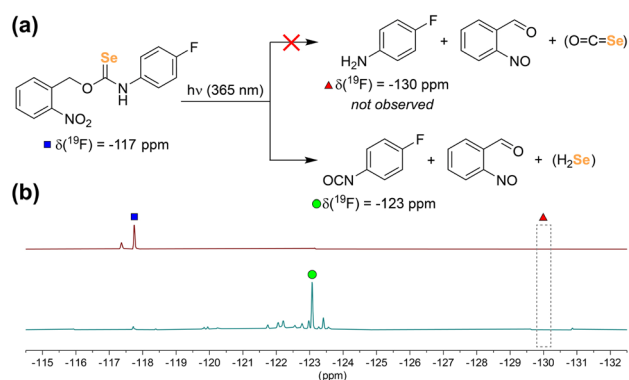
Fig. 3   (a) Chemical reactivity of the PhotoSeCM after irradiation. (b) Stacked ^{19}F NMR spectra of PhotoSeCM before (top) and after (bottom) irradiation. The small peak at −117.4 ppm corresponds to a PhotoSeCM rotamer, as is commonly seen for aryl thio- or selenocarbamates.

fundamentally different than that of the analogous thiocarbamates (*vide infra*).

Building from the PhotoSeCM chemistry, we next wanted to investigate potential COSe/H$_2$Se release from a system that did not require photoactivation. To simplify the activation mechanism, we turned to prior work from our lab on hydrolysis-activated γ-ketothiocarbamates. These systems undergo deprotonation at the β-position to initiate a self-immolative cascade to release COS/H$_2$S and an amine-based payload with reaction rates increasing with increasing pH of solution (Fig. 4a).[35] Moreover, inclusion of the *p*-nitroaniline payload provides a colorimetric response upon donor activation due to the yellow absorbance at 381 nm. To prepare the γ-ketoselenocarbamates, we treated 4-nitrophenyl isoselenocyanate with the desired 4-hydroxybutanone derivative in THF using DBU as a base. We found that the parent compound derived from 4-hydroxybutanone was unstable and could not be isolated, but we were able to prepare the 3-methyl (**1**) and 3,3-dimethyl (**2**) derivates, albeit in low isolated yields (Fig. 4b). The γ-ketoselenocarbamates were isolated as the *O*-alkyl isomers after SiO$_2$ purification, with only minimal Se-alkyl formation that could be removed by purification.

With the γ-ketoselenocarbamate compounds in hand, we next investigated the activation of these donors at different pH values by monitoring the UV-vis spectrum of the released *p*-nitroaniline product. As expected, compound **2**, which lacks deprotonatable hydrogens in the β-position, did not release *p*-nitroaniline, which also supports the general stability of the selenocarbamate motif in solution. Compound **1**, however, did release *p*-nitroaniline as expected, and the rate of release increased at more basic pH values, which is consistent with the expected β-deprotonation mechanism (Fig. 5). Generation of *p*-nitroaniline is consistent with either COSe release followed by rapid hydrolysis or direct release of H$_2$Se, formation of the *p*-nitrophenyl isocyanate, and subsequent hydrolysis. We did not observe the *p*-nitrophenyl isocyanate product directly, but based on the significantly electron withdrawing NO$_2$ group we expect the isocyanate would be rapidly hydrolyzed to *p*-nitroaniline and CO$_2$, especially under basic conditions. In addition to the formation of *p*-nitroaniline, we also observed the precipitation of red Se^0, which is consistent with HSe$^-$ delivery followed by subsequent autooxidation as is common in aqueous solution. We also compared the second order rate constants for donor activation between **1** and the analogous thiocarbamate (γ-KetoTCM-2).[35] We measured *k* values of 0.38(1) M^{-1} s^{-1} and
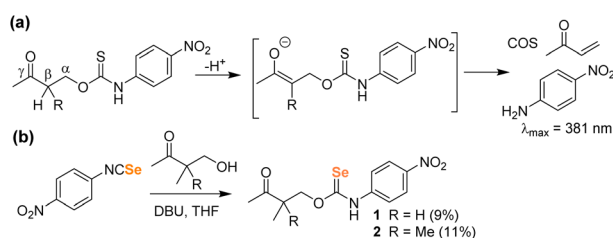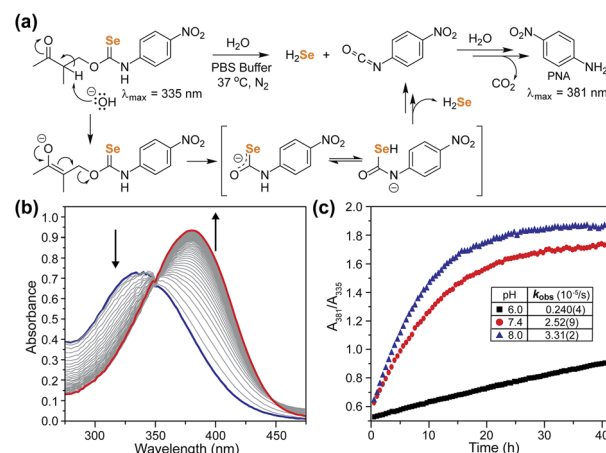

Fig. 5 (a) Proposed reaction mechanism to generate H$_2$Se and PNA, (b) representative UV-vis traces of **1** showing PNA formation in pH 7.4, 10 mM PBS, 37 °C under N$_2$, and (c) plotted absorbance ratio corresponding to PNA formation at different pH values.

0.164(4) M^{-1} s^{-1} for **1** and γ-KetoTCM-2, respectively, which shows a slightly faster rate of release from the Se than the S analogues.

To investigate H$_2$Se release directly, we first attempted a two-step H$_2$Se volatilization experiment using BnBr as an electrophilic trap under anhydrous and anaerobic conditions as was performed previously for acid-activated H$_2$Se donors.[24] Starting with a solution of **1** in DMF, the addition of NaOH resulted in an immediate color change from yellow to red brown, which we attribute to formation of the selenocarbamate intermediate. Upon acidification, we expected to observe H$_2$Se release but instead observed immediate precipitation of elemental Se, which was confirmed by treating the resulting reaction product with PPh$_3$ to form Se=PPh$_3$ (Fig. S18†). After removal of DMF solvent, the resultant ^{1}H NMR spectrum did not show the *p*-nitroaniline product, but rather a new product corresponding to protonated *p*-phenylenediamine, which was confirmed by comparison with the authentic product (Fig. S19†). Based on this observed reactivity, we surmised that the *p*-nitroaniline product was reduced

Fig. 4 (a) COS/H$_2$S release mechanism from γ-ketothiocarbamates after deprotonation at the β-position. (b) Synthesis of γ-ketoselenocarbamates.
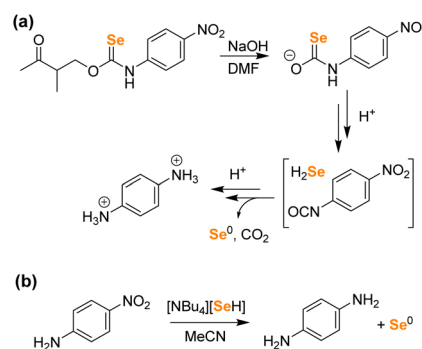

Fig. 6 (a) Observed reactivity of **1** after deprotonation in DMF. Both the *p*-phenylenediamine and Se^0 products were observed by NMR spectroscopy. (b) Treatment of *p*-nitroaniline with HSe$^-$ results in nitro group reduction in organic solution, whereas the reduction in water is inefficient.

by the released HSe⁻ in DMF (Fig. 6). Similar chemical reactivities of H₂Se toward nitroarenes have been previously reported.[42] These results confirm that even in the absence of H₂O, HSe⁻ is released directly, rather than being generated indirectly by the hydrolysis of COSe. To validate the hypothesis that HSe⁻ can reduce nitroaromatics under these conditions, we treated *p*-nitroaniline with [NBu₄][HSe] directly in MeCN, which led to an immediate color change to deep red-brown with precipitation of a red brown solid (Fig. 6). The ¹H NMR spectrum of the product showed clean formation of *p*-phenylenediamine (Fig. S20†), and the ⁷⁷Se NMR spectrum showed consumption of [NBu₄][SeH], indicative of oxidation of HSe⁻ to solid Se⁰ (Fig. S21†). In contrast, treatment of *p*-nitroaniline with [NBu₄][SeH] in aqueous buffer only results in minimal nitro group reduction, which is consistent with the data from Fig. 5. Although Se⁰ formation could potentially be accounted for by the autooxidation of COSe to form CO and Se⁰, the experimental observation of *p*-phenylenediamine formation under the above conditions is most consistent with initial H₂Se release followed by subsequent nitro group reduction with concomitant H₂Se oxidation to Se⁰. Taken together, the above data strongly supports the direct release of H₂Se from selenocarbamates.

Computational investigations

To probe the competing decomposition pathways of selenocarbamates, we performed Density Functional Theory (DFT) calculations using the ωB97X-D functional, the aug-cc-pVDZ basis set for geometry optimizations and frequency calculations, and the SMD implicit solvation model for water. Single-point energy refinements were then obtained using the same functional and solvation model but using the triple-zeta aug-cc-pV(T+d)Z basis set. Full computational details can be found in the ESI.†

Because little is known about the structure of selenocarbamate anions, we first investigated the preferred tautomer of the anionic phenylselenocarbamate **3** as a computational model (Fig. 7). This selenocarbamate intermediate would be the direct structure from which either COSe or HSe⁻ is generated. We find that the NH tautomer (**3a**) is the lowest in energy, and the SeH (**3b**) and OH (**3c**) tautomers are 17.5 and 14.4 kcal mol⁻¹ higher
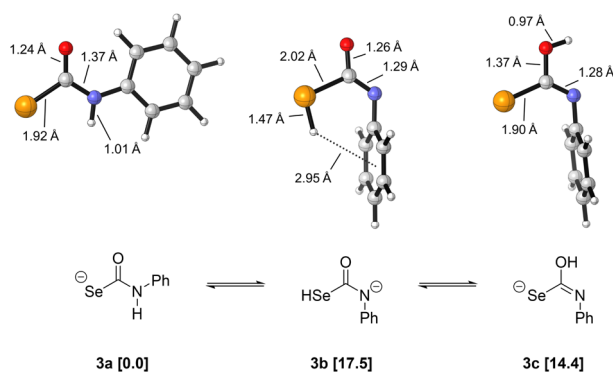
in free energy, respectively. Tautomer **3a** benefits from the stabilization of the negative charge by the most electronegative (O) and most polarizable (Se) atoms, in addition to a flat structure with the phenyl ring *trans* to selenium. In contrast, the most stable conformers of **3b** and **3c** have the Ph group *cis* to selenium, rotated away from the plane of the selenocarbamate. This structure is likely preferred due to strong hyperconjugative interactions between the sp² lone pair of nitrogen and the C–Se σ* acceptor orbital that are in an antiperiplanar arrangement. As expected from the particularly weak H–Se bond (BDE = 66.0 kcal mol⁻¹, lower than H–I = 70.5 kcal mol⁻¹)[43] there is a larger free energy difference between **3b** and **3a** (17.5 kcal-mol⁻¹) than what we computed previously for the NH and SH tautomers in dithiocarbamates (9.7 kcal mol⁻¹).[29]

Our experimental evidence indicates that selenocarbamates like **3** form HSe⁻ directly, but we also investigated the different decomposition pathways of **3** that could result in either COSe or HSe⁻ release to better understand the energetic landscape accessible to selenocarbamates. Starting from **3a**, C–N cleavage could occur directly (**TS1**, Fig. 8), forming COSe and the anilide anion. This pathway has an insurmountable 47.1 kcal mol⁻¹ free energy barrier and is also endergonic by 36.1 kcal mol⁻¹. Despite the expected basicity of anilide in organic solvents, the pK_a of anilide in water is not known. Using DFT, we estimate that protonation of anilide by an isolated water molecule (forming hydroxide and aniline) is only favored by 5.1 kcal mol⁻¹. This small value may be due to the difficulty of modeling proton transfer by DFT and the inaccuracy of treating hydroxide and water using only implicit solvation models. Previous computational work from our group showed that the C–N cleavage pathway of thiocarbamates could be accelerated by the presence of an external acid such as water or dihydrogen phosphate (H₂PO₄⁻).[29] Although there is a slight enthalpic benefit to having an explicit water molecule as an acid mediator to facilitate proton transfer, our calculations for selenocarbamate **3** indicate that there is no free energy benefit and the barrier for **TS1** remains too high to represent a viable reaction pathway (see ESI†). Another scenario is the protonation of **3a** to form a neutral or zwitterionic selenocarbamic acid, from which decomposition to release COSe could occur. The pK_a of selenocarbamic acid has, to the best of our knowledge, never been measured, so we modeled its protonation by water (see ESI†). We find that the barrier for COSe release from a protonated **3a** is at least 22.0 kcal mol⁻¹ and would be higher for more acidic selenocarbamates, such as the *p*-nitro derivative **1**. Such a zwitterionic pathway, however, would be counter to the observed increased rate of product formation at basic pH. Alternatively, elimination of PhNCSe and hydroxide from **3c** has an even larger barrier (53.0 kcal mol⁻¹, see ESI†) than direct COSe extrusion through **TS1**, suggesting that neither of these pathways are operable under normal experimental conditions.

We also investigated the reaction pathway for direct HSe⁻ release from **3**. Although **3b** is the highest-energy tautomer of the selenocarbamate, this tautomer can readily cleave to form HSe⁻ and PhNCO (**TS2**). From **3b**, this TS only requires an additional 4.6 kcal mol⁻¹ and represents a 22.1 kcal mol⁻¹ barrier from the lowest-energy tautomer **3a**. Importantly, **TS2**

Fig. 7 Tautomeric forms and respective free energies (kcal mol⁻¹) of selenocarbamate **3**. Calculations at the ωB97X-D/aug-cc-pVDZ/SMD(water)//ωB97X-D/aug-cc-pV(T+d)Z/SMD(water) level of theory.
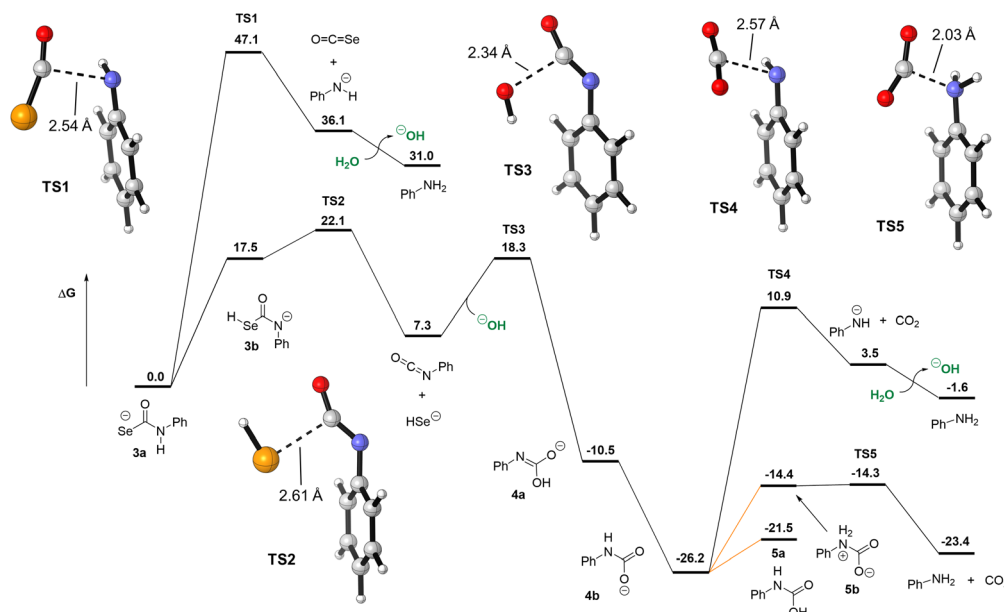
Fig. 8 Decomposition pathways of selenocarbamate **3** comparing COSe and HSe⁻ extrusion pathways. Direct release of HSe⁻ is more energetically favorable than COSe release. Free energies (in kcal mol⁻¹) obtained at the ωB97X-D/aug-cc-pVDZ/SMD(water)//ωB97X-D/aug-cc-pV(T+d)Z/SMD(water) level of theory. Orange lines represent protonation free energies computed from the known pK_a of phenylcarbamic acid in water and assuming a reaction pH of 8 (see ESI†).

only requires tautomerization from **3a** to **3b** and so is not affected by the pK_a of selenocarbamate **3a** in the same way that would be required for elimination of COSe and aniline. This conclusion matches the fact that HSe⁻ generation is the preferred pathway experimentally. Isocyanates, especially those with electron-withdrawing groups, are known to hydrolyze quickly in acidic, basic, or neutral water.[44,45] Using hydroxide as nucleophile, we located **TS3** that has a 11.0 kcal mol⁻¹ barrier from the phenylisocyanate, forming carbamate anion **4a** and its tautomer **4b**, which are 10.5 and 26.2 kcal mol⁻¹ more stable than **3a**, respectively. The activation energy for **TS3** is consistent with the kinetics of hydroxide attack on phenylisocyanate,[45] but might be underestimated for a reaction at pH 8. The mechanism of decarboxylation of carbamates such as **4b** have been studied, and their rates are known to be pH-dependent, with proton transfer to form the key zwitterionic intermediate **5b** being rate-determining.[46] Indeed, direct decarboxylation from the anionic **4b** requires 37.1 kcal mol⁻¹ *via* **TS4**, which is inconsistent with the known reactivity of carbamates. Based on the reported pK_a of **4b** in water (4.62)[46] and a reaction pH of 8, we compute that forming **5a** only requires 4.6 kcal mol⁻¹ and that its zwitterionic tautomer **5b** is 7.2 kcal mol⁻¹ higher in free energy (see ESI for details†). From **5b**, decarboxylation is essentially barrierless, forming the final products aniline and CO₂. For the *p*-nitrophenylcarbamic acid, an intermediate that would be formed in the reaction of **1**, this protonation free energy increases to 9.3 kcal mol⁻¹ by virtue of its lower pK_a of 1.2. Although the decarboxylation would be slower, the hydrolysis of the isocyanate (**TS3**) would in contrast benefit from a higher rate. Similarly, we estimate the pK_a of the *p*-nitrophenyl selenocarbamate to be −1.0 (see ESI†), which would preclude its

protonation under the basic conditions used in this study and as such make the COSe release mechanism even more energetically difficult.

Discussion

The proposed mechanism for direct H₂Se release from selenocarbamates, which is supported by both experimental and computational investigations, differs from the observed prior chemistry with thiocarbamate-based compounds that release COS directly (Fig. 9a). In such systems, direct H₂S release is not observed, but rather COS is the primary product. By contrast, similar selenocarbamate compounds do not release COSe, but rather H₂Se directly (Fig. 9b). These pathway differences may be in part due to inherent bond strength differences in the O–H (carbamate), S–H (thiocarbamate), and Se–H (selenocarbamate) intermediates that significantly impact the tautomerization thermodynamics. This tautomerization may also be reflected in changes in the acidity, which is consistent with the observation that thioamides and thioureas are ~5–6 pK_a units more acidic than their oxygen congeners, which also suggests that Se incorporation may further acidify the chalcogenocarbamate motifs.[47] These factors suggest that the selenocarbamate is less basic than the thiocarbamate, which means that protonation to form the zwitterionic intermediate needed for COSe elimination is less accessible than in the thiocarbamate case, leading to direct HSe⁻ rather than COSe release. In addition, the significant differences in C=O, C=S, and C=Se bond enthalpies mean that the formation is COSe is less favorable than COS or CO₂. Moreover, this observed reactivity is similar to prior work on self-immolative aryl dithiocarbamates, which release H₂S and Ar-NCS directly rather than extruding CS₂ (Fig. 9c).[29] In
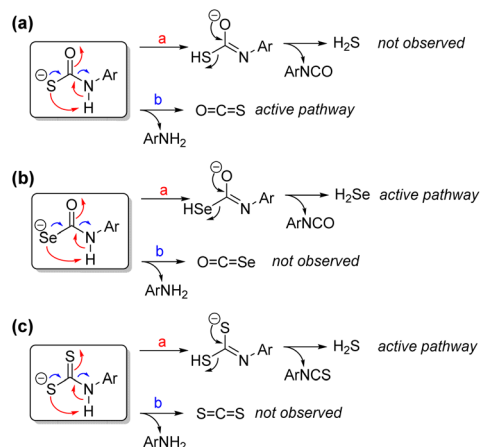
Fig. 9 Possible reaction pathways leading to H_2S/H_2Se and COS/COSe generation from (a) thiocarbamates, (b) selenocarbamates, and (c) dithiocarbamates.

prior work with dithiocarbamates, inclusion of a *para*-nitro group on the aryl payload acidified the dithiocarbamate and increased the efficiency of direct H_2S and isothiocyanate release, which is also consistent with the observed chemistry for the selenocarbamate motifs.

Conclusion

In summary, we show here key differences between the chemistry of thiocarbamates and selenocarbamates with respect to H_2S and H_2Se release. Prior work has established that thiocarbamates readily release COS, which can be quickly hydrolyzed to H_2S by carbonic anhydrases. In contrast, the selenocarbamates investigated in this work release H_2Se directly rather than proceeding through the intermediate release of COSe. This observed reactivity is supported by both experimental and computational investigations. More broadly, the direct release of H_2Se from activatable selenocarbamates may have a higher utility than if COSe were released as an intermediate because the activity of carbonic anhydrases toward COSe as well as the water stability/reactivity of COSe remains unclear. More broadly, this work further highlights that although sulfur and selenium are often described as two of the most similar elements on the periodic table, their fundamental reaction chemistry is significantly different. Understanding these differences are key for both the development of new chemical tools for investigation bioorganic selenium chemistry and also for understanding the chemical underpinnings of why nature has differentiated between these two otherwise similar elements.

Materials and methods

Reagents were purchased from Sigma-Aldrich, Alfa Aesar, or TCI Chemicals and were used directly as received. Deuterated solvents were purchased from Cambridge Isotope Laboratories and used directly as received. [NBu$_4$][SeH] was prepared following literature procedures.[48] ^{1}H, ^{13}C{^{1}H}, ^{19}F, ^{31}P and ^{77}Se NMR spectra were recorded on Bruker 500 and 600 MHz

instruments. Chemical shifts are reported relative to residual protic solvent resonances for ^{1}H and ^{13}C{^{1}H} spectra. All air-free manipulations were performed in an inert atmosphere using standard Schlenk techniques or an Innovative Technologies N$_2$-filled glove box. *Note*: Triphosgene and selenium containing species are toxic and should be handled in a fume hood with appropriate personal protective equipment.

Synthesis

4-Nitrophenyl isoselenocyanate. 4-Nitroformanilide (600 mg, 3.60 mmol) was added to an oven-dried round bottom flask with CH$_2$Cl$_2$ (25 mL), 3 Å molecular sieves, and a stir bar. The flask was capped with a septum, placed on a stir plate, and treated with triethylamine (1.15 mL, 7.60 mmol). The flask was then connected to a reflux condenser, purged with argon, and heated to 45 °C in an oil bath. Once the reaction mixture was brought to reflux, a solution of triphosgene (650 mg, 1.80 mmol) in CH$_2$Cl$_2$ (5.0 mL) was added dropwise over 30 minutes. The reaction mixture was then refluxed for 3 hours, after which selenium powder (710 mg, 9.00 mmol) was added. The reaction mixture was then refluxed overnight and monitored by TLC (3 : 1 hexanes/EtOAc; product R_f = 0.55). The reaction mixture was then removed from the oil bath, allowed to cool to room temperature, filtered through a Celite pad, and concentrated to dryness under vacuum. The resulting crude product was purified by SiO$_2$ column chromatography (gradient of hexanes to 1 : 1 EtOAc/hexanes) to afford a yellow solid (0.571 g, 70%). ^{1}H NMR (600 MHz, CDCl$_3$) δ: 8.26 (d, 2H, J = 8.4 Hz), 8.42 (d, 2H, J = 8.4 Hz). ^{13}C{^{1}H} NMR (151 MHz, CDCl$_3$) δ: 146.2, 135.9, 135.7, 126.9, 125.3. ^{77}Se NMR (115 MHz, CDCl$_3$) δ: −255.9 (s). HRMS m/z [M]$^-$ calcd for [C$_7$H$_4$N$_2$O$_2$Se]$^-$: 227.9438; found 227.9434.

4-Fluorophenyl isoselenocyanate. This compound was prepared as described above for 4-nitrophenyl isoselenocyanate on a 7.40 mmol scale. The product was isolated as a red-orange solid (1.16 g, 78%), with spectroscopic parameters that matched prior literature reports.[49] ^{1}H NMR (600 MHz, CDCl$_3$) δ: 7.28 (m, 2H), 7.07 (m, 2H). ^{13}C{^{1}H} NMR (151 MHz, CDCl$_3$) δ: 161.6 (d, J_{1C-F} = 251 Hz), 130.0, 127.9 (d, J_{3C-F} = 8.8 Hz), 125.9, 116.8 (d, J_{2C-F} = 23 Hz). ^{19}F NMR (564 MHz, CDCl$_3$) δ: −110.2 (m). ^{77}Se NMR (115 MHz, CDCl$_3$) δ: −296.7 (s).

PhotoSeCM. 2-Nitrobenzyl alcohol (153 mg, 1.00 mmol) was added to 12 mL THF in an oven-dried flask under argon and cooled in an ice bath. NaH (60% in paraffin, 120 mg, 3.00 mmol) was added, and then the flask was removed from the ice bath and allowed to warm to room temperature. After 30 min, a solution of 4-fluorophenyl isoselenocyanate (240 mg, 1.20 mmol) in THF (3.00 mL) was added dropwise to the reaction mixture resulting in formation of a deep red colored solution. TLC (1 : 1 EtOAc/hexanes) was used to monitor the reaction over the course of an hour to monitor formation of major *O*-alkyl product (R_f = 0.50) and minor undesired Se-alkyl isomer (R_f = 0.30). Once any formation of Se-alkyl isomer was observed, the reaction mixture was quenched in brine, extracted in EtOAc (3 × 15 mL), dried over MgSO$_4$, filtered, and concentrated to dryness under vacuum to yield the crude product as an orange solid, further recrystallization by layering hexanes over

saturated solution of the crude product in DCM afforded desired product as a white precipitate, which was collected *via* filtration (181 mg, 51%). There are two rotamers of this compound due to slow rotation around the C–N bond, which is also commonly observed for thiocarbamates. Where resolved the two chemical shifts are separated by a "/" for the two rotamer peaks. ^{1}H NMR (600 MHz, DMSO-d_6) δ: 11.96/11.86 (s, 1H), 8.18/8.13 (d, 1H, J = 8.4 Hz), 7.87–7.53 (m, 4H), 7.41/7.39 (d, 1H, J = 8.4 Hz), 7.24/7.19 (t, 2H, J = 8.4 Hz), 6.01/5.92 (s, 2H). ^{13}C{^{1}H} NMR (151 MHz, DMSO-d_6) δ: 188.9, 160.0 (d, J_{1C-F} = 251 Hz), 147.3, 134.2, 133.7, 130.9, 129.5, 129.3, 126.6, 124.7 (d, J_{3C-F} = 8.2 Hz), 115.7 (d, J_{2C-F} = 22 Hz), 72.1. ^{19}F NMR (564 MHz, DMSO-d_6) δ: −116.1 (m). ^{77}Se NMR (115 MHz, DMSO-d_6) δ: 278.3 (s). HRMS m/z [M − H]$^-$ calcd for [C$_{14}$H$_{10}$FN$_2$O$_3$Se]$^-$: 352.9841; found 352.9842.

PNA-MeGKSeCM (1). PNA-NCSe (0.300 g, 1.32 mmol) and THF (20.0 mL) were added to an oven-dried flask and capped with a septum under argon. 4-Hydroxy-3-methyl-2-butanone (148 μL, 1.44 mmol) was added dropwise over 5 minutes. The flask was then wrapped in foil and placed in an ice bath for 20 minutes before DBU (148 μL, 1.00 mmol) was added, which resulted in formation of a red-brown reaction mixture. The reaction mixture was monitored by TLC (1 : 1 hexanes/EtOAc) for 6 hours and then quenched with brine (25 mL). The resulting mixture was extracted with EtOAc (3 × 20 mL), dried over MgSO$_4$, filtered, and concentrated to dryness under vacuum. The resulting crude material was purified *via* SiO$_2$ column chromatography (gradient of hexanes to 1 : 1 hexanes/EtOAc) to afford a yellow-orange solid (37.9 mg, 9%). ^{1}H NMR (600 MHz, DMSO-d_6) δ: 12.16 (s, 1H), 8.21 (d, 2H, J = 9.0 Hz), 7.64 (br m, 2H), 4.70 (m, 2H), 3.17 (m, 1H), 2.19 (s, 3H), 1.14 (d, 3H, J = 7.2 Hz). ^{13}C{^{1}H} NMR (151 MHz, DMSO-d_6) δ: 209.2, 190.9, 143.6, 125.3, 124.7, 121.8, 76.0, 45.0, 28.4, 13.0. ^{77}Se NMR (115 MHz, DMSO-d_6) δ: 350.9 (br s). HRMS m/z [M − H]$^-$ calcd for [C$_{12}$H$_{13}$N$_2$O$_4$Se]$^-$: 329.0041; found 329.0038.

PNA-Me$_2$GKSeCM (2). An identical procedure was followed as for **1** on a 0.25 mmol scale using 4-hydroxy-3,3-dimethyl-2-butanone to afford the product as a yellow solid (9.1 mg, 11%). ^{1}H NMR (600 MHz, DMSO-d_6) δ: 12.17 (s, 1H), 8.22 (d, 2H, J = 9.0 Hz), 7.54 (br s, 2H), 4.65 (br s, 2H), 2.50 (s, 3H), 1.18 (s, 6H). ^{13}C{^{1}H} NMR (151 MHz, DMSO-d_6) δ: 211.4, 191.0, 144.6, 125.2, 122.5, 81.1, 47.9, 25.8, 21.8. ^{77}Se NMR (115 MHz, DMSO-d_6) δ: 352.8 (br s). HRMS m/z [M + H]$^+$ calcd for [C$_{13}$H$_{16}$N$_2$O$_4$Se]$^+$: 345.0354; found: 345.0351.

H$_2$Se release experiments

Photoactivation of PhotoSeCM. PhotoSeCM (15 mg, 0.042 mmol) was dissolved in anhydrous THF (3 mL) in a quartz UV-vis cuvette. This clear solution was irradiated with 365 nm light source during which the initially clear mixture turned yellowish brown with red Se formation, presumably from the auto-oxidation of H$_2$Se. Aliquots of the reaction mixture were analyzed periodically by ^{19}F and ^{77}Se NMR spectroscopy over the course of 72 h, during which PhotoSeCM is gradually converted to the main product *p*-fluoroisocyanate alongside with other minor uncharacterized byproducts. The volatiles were removed

under reduced pressure, and the resulting residue was analyzed by mass spectrometry (Fig. S30†).

Activation of 1 and product analysis. In an N$_2$-filled glovebox, solid NaOH (99 mg, 2.4 mmol) was added to **1** (41 mg, 0.12 mmol) in DMF (1 mL). The solution initially yellow solution turned to deep red, was allowed to stir for 1 h, and was filtered through a pipette filter to remove excess NaOH. The deep red filtrate was transferred to a 5 mL round bottom flask equipped with a stir bar. A small glass vial containing BnBr (15 μL, 0.12 mmol) and K$_2$CO$_3$ (100 mg, 0.73 mmol) was then inserted into the round-bottom flask to trap any volatized H$_2$Se. The flask was then sealed with a rubber septum and excess HCl (2 mL of 1 M HCl in Et$_2$O) was added dropwise *via* syringe, which led to an immediate precipitation of red Se powder. The solution was allowed to stir overnight. The inner vial was removed and the residual solvent in the round-bottom flask was removed under vacuum. The contents of the vial and the flask were both analyzed by NMR spectroscopy. To verify that the red precipitate was Se^0, the insoluble precipitates in the round-bottom flask were treated with PPh$_3$ prior to analysis by ^{31}P NMR spectroscopy.

Reaction of HSe$^-$ with *p*-nitroaniline (PNA). *p*-Nitroaniline (19 mg, 0.14 mmol) in MeCN-d_3 was added to a stirring solution of [NBu$_4$][SeH] (45 mg, 0.14 mmol) in MeCN-d_3, which resulted in formation of a deep red solution. The reaction mixture was stirred for 1 h prior to analysis by ^{1}H and ^{77}Se NMR spectroscopy, which revealed consumption of HSe$^-$ and reduction of the PNA product.

Computational studies

Gaussian 16 was used to perform Density Functional Theory (DFT) calculations, where geometry optimizations were conducted with the ωB97X-D method using the aug-cc-pVDZ basis set. Following this, single-point energy refinements were performed using the ωB97X-D functional and the aug-cc-pV(T+d)Z basis set. The SMD implicit solvation model for water was used at all stages to consider solvation effects. The final free energies were computed by adding the free energy corrections obtained from the frequency analysis to the single-point electronic energies. Full computational details are provided in the ESI.†

Data availability

Experimental and computational data are included in the ESI.†

Author contributions

MDP and PAC supervised this work. TDN and KL synthesized and characterized all compounds and made experimental measurements. JS and PAC carried out computational investigations and analysis. TDN, KL, JS, PAC, and MDP wrote the manuscript.

Conflicts of interest

There are no conflicts to declare.

Acknowledgements

Notes and references

1 M. R. Filipovic, J. Zivanovic, B. Alvarez and R. Banerjee, *Chem. Rev.*, 2018, **118**, 377–461.

2 L. Liaudet, F. G. Soriano and C. Szabo, *Crit. Care Med.*, 2000, **28**, N37–N52.

3 S. W. Ryter and L. E. Otterbein, *BioEssays*, 2004, **26**, 270–280.

4 R. Wang, *Physiol. Rev.*, 2012, **92**, 791–896.

5 D. A. Wink and J. B. Mitchell, *Free Radical Biol. Med.*, 1998, **25**, 434–456.

6 L. Y. Wu and R. Wang, *Pharmacol. Rev.*, 2005, **57**, 585–630.

7 X. Q. Chen, X. Z. Tian, I. Shin and J. Yoon, *Chem. Soc. Rev.*, 2011, **40**, 4783–4804.

8 V. S. Lin and C. J. Chang, *Curr. Opin. Chem. Biol.*, 2012, **16**, 595–601.

9 C. R. Powell, K. M. Dillon and J. B. Matson, *Biochem. Pharmacol.*, 2018, **149**, 110–123.

10 C. M. Levinn, M. M. Cerda and M. D. Pluth, *Antioxid. Redox Signaling*, 2020, **32**, 96–109.

11 P. G. Wang, M. Xian, X. P. Tang, X. J. Wu, Z. Wen, T. W. Cai and A. J. Janczuk, *Chem. Rev.*, 2002, **102**, 1091–1134.

12 T. Nagano and T. Yoshimura, *Chem. Rev.*, 2002, **102**, 1235–1269.

13 X. Y. Ji, K. Damera, Y. Q. Zheng, B. C. Yu, L. E. Otterbein and B. H. Wang, *J. Pharm. Sci.*, 2016, **105**, 406–416.

14 C. C. Romao, W. A. Blattler, J. D. Seixas and G. J. L. Bernardes, *Chem. Soc. Rev.*, 2012, **41**, 3571–3583.

15 K. A. Cupp-Sutton and M. T. Ashby, *Antioxidants*, 2016, **5**, 42.

16 M. Roman, P. Jitaru and C. Barbante, *Metallomics*, 2014, **6**, 25–54.

17 C. Hartmann, B. Nussbaum, E. Calzia, P. Radermacher and M. Wepler, *Front. Physiol.*, 2017, **8**, 691.

18 M. Kuganesan, K. Samra, E. Evans, M. Singer and A. Dyson, *Intensive Care Med. Exp.*, 2019, **7**, 71.

19 X. Y. Kang, H. J. Huang, C. Y. Jiang, L. H. Cheng, Y. Q. Sang, X. K. Cai, Y. L. Dong, L. Sun, X. Wen, Z. Xi and L. Yi, *J. Am. Chem. Soc.*, 2022, **144**, 3957–3967.

20 D. Kang, J. Lee, C. Wu, X. Guo, B. J. Lee, J. S. Chun and J. H. Kim, *Exp. Mol. Med.*, 2020, **52**, 1198–1208.

21 C. Szabo and A. Papapetropoulos, *Pharmacol. Rev.*, 2017, **69**, 497–564.

22 L. Li, M. Whiteman, Y. Y. Guan, K. L. Neo, Y. Cheng, S. W. Lee, Y. Zhao, R. Baskar, C. H. Tan and P. K. Moore, *Circulation*, 2008, **117**, 2351–2360.

23 W. Feng, X. Y. Teo, W. Novera, P. M. Ramanujulu, D. Liang, D. J. Huang, P. K. Moore, L. W. Deng and B. W. Dymock, *J. Med. Chem.*, 2015, **58**, 6456–6480.

24 T. D. Newton and M. D. Pluth, *Chem. Sci.*, 2019, **10**, 10723–10727.

25 T. D. Newton, S. G. Bolton, A. C. Garcia, J. E. Chouinard, S. L. Golledge, L. N. Zakharov and M. D. Pluth, *J. Am. Chem. Soc.*, 2021, **143**, 19542–19550.

26 R. A. Hankins, M. E. Carter, C. L. Zhu, C. Chen and J. C. Lukesh, *Chem. Sci.*, 2022, **13**, 13094–13099.

27 A. K. Steiger, Y. Zhao and M. D. Pluth, *Antioxid. Redox Signaling*, 2018, **28**, 1516–1532.

28 Y. Zhao and M. D. Pluth, *Angew. Chem., Int. Ed.*, 2016, **55**, 14638–14642.

29 Y. Zhao, H. A. Henthorn and M. D. Pluth, *J. Am. Chem. Soc.*, 2017, **139**, 16365–16376.

30 Y. M. Hu, X. Y. Li, Y. Fang, W. Shi, X. H. Li, W. Chen, M. Xian and H. M. Ma, *Chem. Sci.*, 2019, **10**, 7690–7694.

31 C. L. Zhu, S. I. Suarez and J. C. Lukesh, *Tetrahedron Lett.*, 2021, **69**, 152944.

32 Y. Zhao, S. G. Bolton and M. D. Pluth, *Org. Lett.*, 2017, **19**, 2278–2281.

33 A. K. Sharma, M. Nair, P. Chauhan, K. Gupta, D. K. Saini and H. Chakrapani, *Org. Lett.*, 2017, **19**, 4822–4825.

34 P. Stacko, L. Muchova, L. Vitek and P. Klan, *Org. Lett.*, 2018, **20**, 4907–4911.

35 Y. Zhao, A. K. Steiger and M. D. Pluth, *Angew. Chem., Int. Ed.*, 2018, **57**, 13101–13105.

36 A. K. Gilbert, Y. Zhao, C. E. Otteson and M. D. Pluth, *J. Org. Chem.*, 2019, **84**, 14469–14475.

37 P. Chauhan, P. Bora, G. Ravikumar, S. Jos and H. Chakrapani, *Org. Lett.*, 2017, **19**, 62–65.

38 A. K. Steiger, M. Marcatti, C. Szabo, B. Szczesny and M. D. Pluth, *ACS Chem. Biol.*, 2017, **12**, 2117–2123.

39 C. Y. Zhang, Q. Z. Zhang, K. Zhang, L. Y. Li, M. D. Pluth, L. Yi and Z. Xi, *Chem. Sci.*, 2019, **10**, 1945–1952.

40 K. Eriksen, A. Ulfkjaer, T. I. Solling and M. Pittelkow, *J. Org. Chem.*, 2018, **83**, 10786–10797.

41 A. Sorensen, B. Rasmussen, S. Agarwal, M. Schau-Magnussen, T. I. Solling and M. Pittelkow, *Angew. Chem., Int. Ed.*, 2013, **52**, 12346–12349.

42 T. Miyata, K. Kondo, S. Murai, T. Hirashima and N. Sonoda, *Angew. Chem., Int. Ed. Engl.*, 1980, **19**, 1008.

43 *Lange's Handbook of Chemistry*, McGraw-Hill Education, New York, 17th edn, 2017.

44 A. F. Hegarty, C. N. Hegarty and F. L. Scott, *J. Chem. Soc., Perkin Trans. 2*, 1975, 1166–1171.

45 E. A. Castro, R. B. Moodie and P. J. Sansom, *J. Chem. Soc., Perkin Trans. 2*, 1985, 737–742.

46 S. L. Johnson and D. L. Morrison, *J. Am. Chem. Soc.*, 1972, **94**, 1323–1334.

47 F. G. Bordwell, *Acc. Chem. Res.*, 1988, **21**, 456–463.

48 H. A. Fargher, N. Lau, L. N. Zakharov, M. M. Haley, D. W. Johnson and M. D. Pluth, *Chem. Sci.*, 2019, **10**, 67–72.

49 D. H. R. Barton, S. I. Parekh, M. Tajbakhsh, E. A. Theodorakis and C. L. Tse, *Tetrahedron*, 1994, **50**, 639–654.